Spectrally-efficient all-optical OFDM by WSS and AWG

J. Hoxha,[1,*] J. Morosi,[2] S. Shimizu,[3] P. Martelli,[2] P. Boffi,[2] N. Wada,[3] and G. Cincotti[1]

[1]*University Roma Tre, Engineering Department, via Vito Volterra 62, I-00146 Rome, Italy*
[2]*Politecnico di Milano, Dept. Electronics Information and Bioengeneering, via G. Ponzio34/5, 20133 Milan, Italy*
[3]*National Institute of Information and Communications Technology (NICT), Tokyo, Japan*
[*]*julian.hoxha@uniroma3.it*

Abstract: We report on the transmission experiment of seven 12.5-GHz spaced all optical-orthogonal frequency division multiplexed (AO-OFDM) subcarriers over a 35-km fiber link, using differential quadrature phase shift keying (DQPSK) modulation and direct detection. The system does not require chromatic dispersion compensation, optical time gating at the receiver (RX) or cyclic prefix (CP), achieving the maximum spectral efficiency. We use a wavelength selective switch (WSS) at the transmitter (TX) to allow subcarrier assignment flexibility and optimal filter shaping; an arrayed waveguide grating (AWG) AO-OFDM demultiplexer is used at the RX, to reduce the system cost and complexity.

OCIS codes: (060.2330) Fiber optics communications; (060.5060) Phase modulation; (060.4230) Multiplexing.

References and links

1. R. W. Tkach, "Scaling optical communications for the next decade and beyond," Bell Labs Tech. J. **14**(4), 3–9 (2010).
2. S. Chandrasekhar and X. Liu, "Advances in Tb/s superchannels," in Systems and Networks, Vol. VIB of Optical Fiber Telecommunications (2013), pp. 83–117.
3. O. Gerstel, M. Jinno, A. Lord, and S. B. Yoo, "Elastic optical networking: A new dawn for the optical layer?" IEEE Commun. Mag. **50**(2), 12–20 (2012).
4. Y. K. Huang, E. Ip, Z. Wang, M. F. Huang, Y. Shao, and T. Wang, "Transmission of spectral efficient super-channels using all-optical OFDM and digital coherent receiver technologies," J. Lightwave Technol. **29**(24), 3838–3844 (2011).
5. K. Lee, C. T. D. Thai, and J.-K. K. Rhee, "All optical discrete Fourier transform processor for 100 Gbps OFDM transmission," Opt. Express **16**(6), 4023–4028 (2008).
6. A. Sano, E. Yamada, H. Masuda, E. Yamazaki, T. Kobayashi, E. Yoshida, Y. Miyamoto, R. Kudo, K. Ishihara, and Y. Takatori, "No-guard-interval coherent optical OFDM for 100-Gb/s long-haul WDM transmission," J. Lightwave Technol. **27**(16), 3705–3713 (2009).
7. D. Hillerkuss, R. Schmogrow, T. Schellinger, M. Jordan, M. Winter, G. Huber, T. Vallaitis, R. Bonk, P. Kleinow, F. Frey, M. Roeger, S. Koenig, A. Ludwig, A. Marculescu, J. Li, M. Hoh, M. Dreschmann, J. Meyer, S. Ben Ezra, N. Narkiss, B. Nebendahl, F. Parmigiani, P. Petropoulos, B. Resan, A. Oehler, K. Weingarten, T. Ellermeyer, J. Lutz, M. Moeller, M. Huebner, J. Becker, C. Koos, W. Freude, and J. Leuthold, "26 Tbit s^{-1} line-rate super-channel transmission utilizing all-optical fast Fourier transform processing," Nat. Photonics **5**(6), 364–371 (2011).
8. D. Hillerkuss, M. Winter, M. Teschke, A. Marculescu, J. Li, G. Sigurdsson, K. Worms, S. Ben Ezra, N. Narkiss, W. Freude, and J. Leuthold, "Simple all-optical FFT scheme enabling Tbit/s real-time signal processing," Opt. Express **18**(9), 9324–9340 (2010).
9. T. Sakamoto, T. Kawanishi, and M. Izutsu, "Asymptotic formalism for ultraflat optical frequency comb generation using a Mach-Zehnder modulator," Opt. Lett. **32**(11), 1515–1517 (2007).
10. Z. Wang, K. S. Kravtsov, Y. K. Huang, and P. R. Prucnal, "Optical FFT/IFFT circuit realization using arrayed waveguide gratings and the applications in all-optical OFDM system," Opt. Express **19**(5), 4501–4512 (2011).
11. A. J. Lowery, "Design of Arrayed-Waveguide Grating Routers for use as optical OFDM demultiplexers," Opt. Express **18**(13), 14129–14143 (2010).
12. S. Shimizu, G. Cincotti, and N. Wada, "Demonstration of 8 x 12.5 Gbit/s all-optical OFDM system with an arrayed waveguide grating and waveform reshaping," in Proc. European Conference on Optical Communication 2012 (ECOC2012), paper Th.1.A.2 (2012).
13. S. Shimizu, G. Cincotti, and N. Wada, "Analysis of frequency mismatch in all-optical OFDM systems," in Proceedings of the Conference on Photonics in Switching 2012 (PS2012), paper Th-S15–O11 (2012).

#233594 - $15.00 USD Received 29 Jan 2015; revised 30 Mar 2015; accepted 31 Mar 2015; published 20 Apr 2015

14. S. Shimizu, G. Cincotti, and N. Wada, "Demonstration and performance investigation of all-optical OFDM systems based on arrayed waveguide gratings," Opt. Express **20**(26), B525–B534 (2012).
15. S. Shimizu, G. Cincotti, and N. Wada, "Chromatic dispersion monitoring and adaptive compensation using pilot symbols in an 8 x 12.5 Gbit/s all-optical OFDM system," Opt. Express **22**(7), 8734–8741 (2014).
16. A. J. Lowery, "Inserting a cyclic prefix using Arrayed-Waveguide Grating Routers in all-optical OFDM transmitters," Opt. Express **20**(9), 9742–9754 (2012).
17. P. Zakynthinos, G. Cincotti, M. Nazarathy, R. Kaiser, P. Bayvel, R. I. Killey, M. Angelou, S. B. Ezra, M. Irion, A. Tomalchev, B. Gomez Saavedra, J. Hoxha, V. Grundlehner, N. Psaila, G. Vollrah, R. Magri, G. Papastergiou, and I. Tomkos, "Advanced hybrid integrated transceivers to realize flexible Terabit networking," Photonics. Soc. Newsletter **28**(1), 12–19 (2014).
18. H. Chen, M. Chen, and S. Xie, "All-optical sampling orthogonal frequency-division multiplexing scheme for high-speed transmission system," J. Lightwave Technol. **27**(21), 4848–4854 (2009).
19. L. B. Du, J. Schroeder, M. M. Morshed, B. Eggleton, and A. J. Lowery, "Optical inverse Fourier transform generated 11.2-Tbit/s no-guard-interval all-optical OFDM transmission," in Proc. Optical Fiber Communication Conference 2013 (OFC2013), paper OW3B.5 (2013).
20. L. B. Du, J. Schroeder, J. Carpenter, B. Eggleton, and A. J. Lowery, "Flexible all-optical OFDM using WSSs," in Proc. Optical Fiber Communication Conference 2013 (OFC2013), paper PDP5B.9 (2013).
21. X. Wang, N. Wada, N. Kataoka, T. Miyazaki, G. Cincotti, and K. Kitayama, "100km field trial of 1.24 Tbit/s, spectral efficient, asynchronous 5 WDMX25 DPSK-OCDMA using one set of 50X50 ports large scale en/decoder," in Proc. Optical Fiber Communication Conference 2007 (OFC2007), paper PDP14.
22. N. Kataoka, N. Wada, G. Cincotti, and K.-i. Kitayama, "2.56 Tbps (40-Gbps x 8-wavelength x 4-OC x 2-POL) asynchronous WDM-OCDMA-PON using a multi-port encoder/decoder," in Proc. Optical Fiber Communication Conference 2011 (ECOC2011), paper Th.13.B.6.
23. G. Cincotti, "Enhanced functionalities of AWGs," J. Lightwave Technol. **33**(5), 998–1006 (2015).
24. H. Sanjoh, E. Yamada, and Y. Yoshikuni, "Optical orthogonal frequency division multiplexing using frequency/time domain filtering for high spectral efficiency up to 1 bit/s/Hz" in Proceedings of OFC 2002 (2002), pp. 401–402.
25. J. Schroder, L. B. Du, J. Carpenter, B. J. Eggleton, and A. J. Lowery, "All-optical OFDM with cyclic prefix insertion using flexible wavelength selective switch optical processing," J. Lightwave Technol. **32**(4), 752–759 (2014).
26. G. Cincotti, N. Wada, S. Yoshima, N. Kataoka, and K.-i. Kitayama, "200Gchip/s, 16-label simultaneous multiple-optical encoder/decoder and its application to optical packet switching," in Proc. Optical Fiber Communications Conference 2005 (OFC2005), paper PDP37 (2005).
27. I. Kang, M. Rasras, X. Liu, S. Chandrasekhar, M. Cappuzzo, L. T. Gomez, Y. F. Chen, L. Buhl, S. Cabot, and J. Jaques, "All-optical OFDM transmission of 7 x 5-Gb/s data over 84-km standard single-mode fiber without dispersion compensation and time gating using a photonic-integrated optical DFT device," Opt. Express **19**(10), 9111–9117 (2011).
28. I. Morohashi, T. Sakamoto, H. Sotobayashi, T. Kawanishi, I. Hosako, and M. Tsuchiya, "Widely repetition-tunable 200 fs pulse source using a Mach-Zehnder-modulator-based flat comb generator and dispersion-flattened dispersion-decreasing fiber," Opt. Lett. **33**(11), 1192–1194 (2008).
29. A. J. Lowery, J. Schröder, and L. B. Du, "Flexible all-optical frequency allocation of OFDM subcarriers," Opt. Express **22**(1), 1045–1057 (2014).
30. L. B. Du and A. J. Lowery, "The validity of "Odd and Even" channels for testing all-optical OFDM and Nyquist WDM long-haul fiber systems," Opt. Express **20**(26), B445–B451 (2012).

1. Introduction

With the increasing demand for high data-rate telecom services, optical networks are requested to provide enhanced bandwidth management flexibility, as well as high spectral efficiency [1–3]. All-optical orthogonal frequency division multiplexing (AO-OFDM) is a promising approach for next-generation high-speed elastic networks, where the subcarriers multiplexing and de-multiplexing is performed in the optical domain, with reduced power consumption [4–7]. In addition, AO-OFDM schemes overcome the electronic bottleneck, related to the processing speed for the inverse fast Fourier transform/fast Fourier transform (IFFT/FFT), and to the digital to analog converter bandwidth [8].

To optically generate AO-OFDM subcarriers, a flat and stable optical comb is needed to ensure channels orthogonality, that can be obtained using a single light source, a dual-drive Mach-Zehnder modulator (DD-MZM), and an optical phase modulator (PM) [9].

Many different approaches have been presented in literature to optically shape the input light source with a frequency *sinc*-like profile, and generate the AO-OFDM subcarriers; the optical implementations of the IFFT/FFT schemes are based on trees of Mach Zehnder delay interferometers (MZDI) [7,8], arrayed waveguide gratings (AWG) [10–17], fiber Bragg gratings (FBG) [18], and wavelength selective switches (WSS) [19, 20]. The first approach is not scalable, as the number of MZDIs required for a *N*-channel multiplexer/demultiplexer is

#233594 - $15.00 USD Received 29 Jan 2015; revised 30 Mar 2015; accepted 31 Mar 2015; published 20 Apr 2015

N-1; in addition, that scheme requires thermal phase shifters, that increases the cost and complexity of the device. A single FBG can implement a *sinc*-shaped optical filter, and *N* different devices are required in a *N*-channel AO-OFDM system, both at the transmitter (TX) and receiver (RX). On the other hand, the AWG is a planar device that can generate and process up to $N = 50$ subcarriers in parallel, in a complete passive way [21, 22], in addition, it can be integrated with modulators or photodetectors in Tb-capable transceivers [17]. The main limitation for the use of an AWG in an AO-OFDM system is the slab-diffraction effect, that affects the rectangular time waveform; however, this impairment can be compensated by an external modulator [12], or by a suitable tapering in the slab coupler [23]. To achieve a flexible bandwidth management, the OFDM subcarriers should be arbitrary assigned, and for this reason, we replace the AWG with a WSS at the TX. The WSS presents a lower frequency resolution than an AWG, but the channel assignment can be varied by programming the filter responses.

In a conventional OFDM scheme, channel orthogonality is achieved only at the time instant that corresponds to the center of the auto- and cross-correlation time waveforms, and time-gating is applied to reduce the interchannel interference (ICI) [24]. However, when an optical OFDM superchannel is transmitted over an uncompensated link, the OFDM subcarriers experience different delays and time-gating is no longer efficient to suppress ICI; different approaches have been proposed in literature to overcome this limitation either using monitoring techniques [15], or introducing a cyclic prefix (CP) [16, 25], that reduces the overall spectral efficiency. In the present paper, we numerically and experimentally demonstrate that using a suitable filter shaping at the TX, all the OFDM subcarriers are successfully received, without CP, or chromatic dispersion (CD) compensation, or optical time gating. Seven AO-OFDM subcarriers are transmitted over a fiber span, allowing an effective bandwidth sharing among different users, without reducing the spectral efficiency that is 2 bit/s/Hz. In addition, the RX is largely simplified, and real-time OFDM signal processing is achieved.

An 8-channel 12.5-GHz spaced OFDM system has been already experimentally demonstrated, using an AWG both at TX and RX [15]. In that case, CD largely affects the system performances, and a maximum transmission distance of 15 Km was achieved in an uncompensated link. In the present paper, we demonstrate that the combined use of a WSS, with a second-order super-Gaussian transfer function, and an AWG allows us to extend the distance up to 35-km. We also observe that the electrical signal shape does not affect the system performances, because the optical signal is a train of Gaussian pulses with 13-ps full width at half maximum (FWHM) and the electrical signal has 80 ps duration (bit rate $B = 12.5$ GHz), that is six-times larger.

The WSS and AWG performances are theoretically and numerically analyzed in Section 2. We demonstrate that the proposed scheme yields a lower ICI, with respect to a conventional scheme where two AWGs are used; Gaussian superchannels are also considered for comparison. Section 3 is devoted to the description of the system setup and the experimental results. BER measures for directly-detected differential quadrature phase shift keying

#233594 - $15.00 USD Received 29 Jan 2015; revised 30 Mar 2015; accepted 31 Mar 2015; published 20 Apr 2015

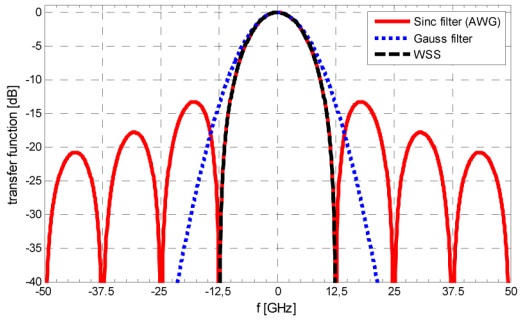

Fig. 1. Simulated transfer functions of *sinc*-shaped, Gaussian and WSS filters.

(DQPSK)-modulated subcarriers are reported. The results in back-to-back (B2B) are shown together with the performance achieved with quadrature phase shift keying (QPSK) modulation and coherent detection, to demonstrate the effectiveness of the proposed AO-OFDM transmitter. Finally, error-free propagation for different fiber link lengths is demonstrated.

2. WSS and AWG performance

Figure 1 shows the simulated transfer function of an AWG that optically performs the IFFT/FFT of a signal at symbol rate B = 12.5 Gb/s; the filter has a *sinc* shape, the 3-dB bandpass bandwidths is 11 GHz and the side-lobe peak is 13.3 dB lower than the main lobe.

The OFDM symbol corresponding to the m-th subcarrier (m = 0,1,..N-1), has a rectangular profile in the time-domain, with duration $T = 1/B$, that equates the inverse of the symbol rate

$$h_m(t) = \frac{1}{\sqrt{T}}\mathrm{rect}\left(\frac{t}{T}\right)e^{j2\pi\frac{mt}{T}} = \begin{cases} \dfrac{e^{j2\pi\frac{mt}{T}}}{\sqrt{T}} & 0 < t < T \\ 0 & otherwise \end{cases} \quad m = 0,1,..N-1. \tag{1}$$

The autocorrelation function, detected at the AWG matched port at the RX (i.e. the port that corresponds to the transmitted subcarrier), has a triangular shape with duration twice of the symbol length, that is shown in Fig. 2(a) [26].

The crosscorrelation among two different subcarriers can be evaluated as

$$\begin{aligned} h_m(t) * h_n(t) &= \frac{1}{T}\int_{-\infty}^{\infty}\mathrm{rect}\left(\frac{t-\tau}{T}\right)\mathrm{rect}\left(\frac{\tau}{T}\right)e^{j2\pi\frac{n(t-\tau)}{T}}e^{j2\pi\frac{m\tau}{T}}d\tau \\ &= \frac{e^{j\pi\frac{(m+n)t}{T}}}{\pi(m-n)}\sin\left[\pi(m-n)\left(\frac{1-|t|}{T}\right)\right]\mathrm{rect}\left(\frac{t}{2T}\right), \qquad m \neq n \quad m,n = 0,1,..N-1 \end{aligned} \tag{2}$$

and is plotted in Fig. 2(b) for adjacent subcarriers (m-n = 1) that generate the largest crosstalk. Thanks to the subcarrier orthogonality, the crosscorrelation signal is zero for t = 0, that corresponds to the maximum of the autocorrelation signal. When CD is completely compensated, time gating is applied at instant t = 0, and ICI is eliminated. However, in an

#233594 - $15.00 USD Received 29 Jan 2015; revised 30 Mar 2015; accepted 31 Mar 2015; published 20 Apr 2015

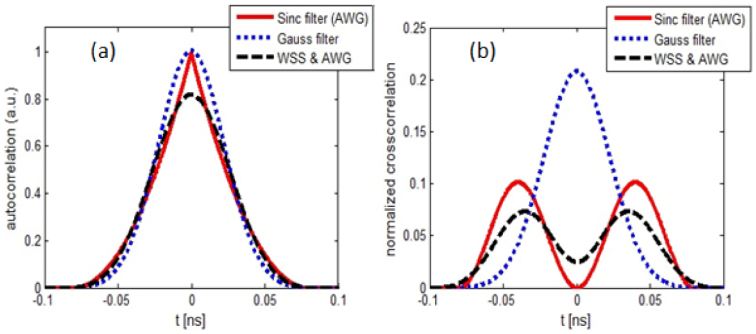

Fig. 2. Numerical simulations of a multichannel system with an AWG (*sinc*-shaped filter of AO-OFDM) at TX and RX (full line), Gaussian filters at TX and RX (dotted line) and a WSS at the TX and an AWG at the RX (dashed line). (a) Autocorrelation. (b) Crosscorrelation of adjacent subcarriers (m-n = 1).

uncompensated link, the OFDM subcarriers experience different delays and the orthogonality condition is no longer satisfied. In this case, time gating cannot completely remove ICI, that is evaluated in the worst case condition, as the ratio between the square modulus of the crosscorrelation peak (CCP = $1/\pi^2 = 0.1$) for m-n = 1 (adjacent subcarriers) that occurs at $t = \pm T/2$, and the power of the autocorrelation peak (ACP) (that has been normalized and is equal to 1) [27]. Therefore in the case of an uncompensated link, it is ICI = –9.94 dB.

The autocorrelation function has duration $2T$, that is double with respect to the OFDM symbol length. Therefore, two consecutive received symbols partially overlap and the intersymbol interference (ISI) can be estimated as the ratio between the square modulus of the autocorrelation function at instant $t = T/2$ (crossing point of two autocorrelation functions corresponding to two consecutive symbols) that is 0.25, and the ACP. Then ISI = –6 dB.

To make a comparison, we consider a multichannel system, where the *sinc*-shaped filters of an AO-OFDM are replaced by Gaussian subcarriers, spaced of $B = 1/T$. In this case, the transmitted symbol has a Gaussian shape in the time domain, that has been normalized, so that the average transmitted power is equal to 1

$$h'_m(t) = \frac{1}{\sqrt[4]{\pi\delta_t^2}} e^{-\frac{t^2}{2\delta_t^2}} e^{j2\pi\frac{mt}{T}} \qquad m = 0,1,..N-1. \tag{3}$$

The variance $\delta_t^2 = \ln(4)/(\pi\,\Delta f)^2$ is related to the 3dB filter passband Δf. The autocorrelation function

$$h'_m(t) * h'_m(t) = e^{-\frac{t^2}{4\delta_t^2}} e^{j2\pi\frac{mt}{T}} \qquad m = 0,1,..N-1 \tag{4}$$

is plotted in Fig. 2(a), and, also in this case, it is ACP = 1. To make a fair comparison with the AO-OFDM system, where the transmitted symbols have a rectangular profile with duration $T = 1/B$, we set $\delta_t = T\Big/\left(2\sqrt{\pi}\right)$. Therefore, both rectangular and Gaussian symbols have the same mean value in the time domain, and their corresponding filter functions assume the same

#233594 - $15.00 USD Received 29 Jan 2015; revised 30 Mar 2015; accepted 31 Mar 2015; published 20 Apr 2015

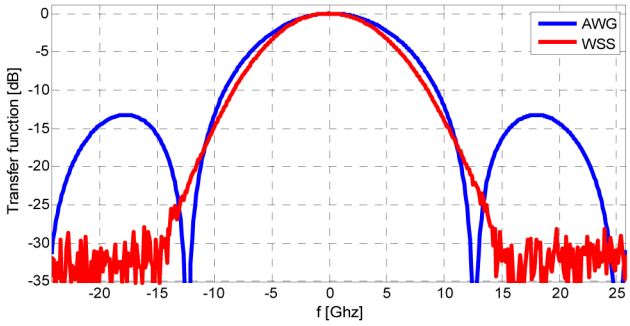

Fig. 3. Measured WSS transfer function and numerical simulation of the AWG transfer function.

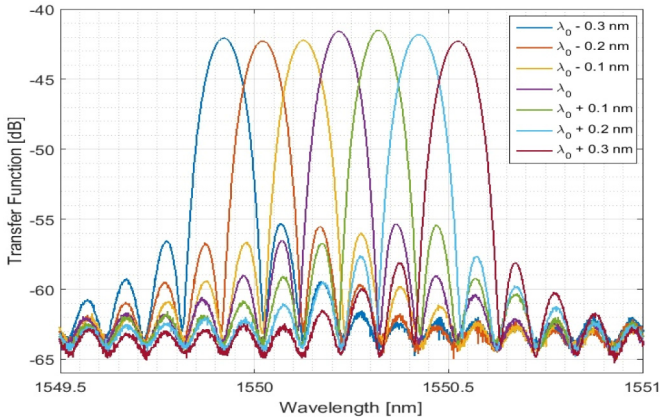

Fig. 4. Measured 7-channel spectra at the AWG outputs.

value at the central frequency $f = 0$. The Gaussian filter function is shown in Fig. 1 and the corresponding 3-dB bandwidth is $\Delta f = 2B\sqrt{\ln 2/\pi} = 11.74\text{GHz}$.

The crosscorrelation of two Gaussian symbols transmitted over two different subcarriers is

$$h'_m(t) * h'_n(t) = \int_{-\infty}^{\infty} e^{-\frac{\tau^2}{2\delta_t^2}} e^{-\frac{(t-\tau)^2}{2\delta_t^2}} e^{j2\pi\frac{m\tau}{T}} e^{j2\pi\frac{n(t-\tau)}{T}} d\tau$$
$$= e^{-\frac{\pi^2\delta_t^2(m-n)^2}{T^2}} e^{-\frac{t^2}{4\delta_t^2}} e^{j2\pi\frac{m+n}{T}t} \quad m \neq n \quad m,n = 0,1,..N-1 \tag{5}$$

and, for m-n = 1, CCP = $e^{-\frac{2\pi^2\delta_t^2}{T^2}}$. The peak of the crosscorrelation signal occurs at $t = 0$, and it overlaps with the ACP, so that in this case time-gating cannot eliminate ICI even when CD is compensated, because Gaussian subcarrier are not orthogonal. In our example CCP = $e^{-\frac{\pi}{2}}$ = 0.21 and ICI = –6.82 dB.

From an inspection of Fig. 2(b), it is evident that ICI in a Gaussian superchannel is almost the double of that one of AO-OFDM subcarriers transmitted over an uncompensated link, in the case that the two systems have the same 3dB bandwidth Δf. On the other hand, ISI is almost the same in both cases, as it is shown in Fig. 2(a).

#233594 - $15.00 USD Received 29 Jan 2015; revised 30 Mar 2015; accepted 31 Mar 2015; published 20 Apr 2015

To reduce ICI without affecting other system performance, we apply a filter function at the transmitter that eliminates all the sidelobes of the *sinc*-function, as shown in Fig. 1. In our experiment, we programmed a WSS with a second-order super-Gaussian shape, that is shown in Fig. (3); the 3dB and 6dB bandwidths are 9.8 GHz and 13 GHz, respectively. The numerically simulated AWG transfer function is also shown for reference in Fig. (3), whereas Fig. (4) reports the measured spectra at the AWG outputs.

The autocorrelation and crosscorrelation function of a system having a WSS at the TX and an AWG at the RX are shown in Fig. 2(a) and 2(b), respectively. In this case, ACP = 0.82 and CCP = 0.074, respectively, and ICI is reduced to −10.45 dB in an uncompensated link.

Therefore, the proposed system largely reduces the overall ICI when optical time gating is not applied and CD is not compensated. Of course, a suitable bandwidth is required at the RX side to sample in the middle of the eye diagram. The use of a WSS in the TX allows bandwidth management flexibility, as different subcarriers can be easily assigned by programming the WSS. On the other hand, only an AWG can generate a *sinc*-shaped filter with high resolution, and demultiplex a large number of AO-OFDM subcarriers.

3. Experimental setup and results

Figure 5 shows the TX architecture for a 7-channel DQPSK-modulated AO-OFDM system; the subcarrier spacing equates the symbol rate B = 12.5 GHz, to achieve the maximum spectral efficiency.

The optical comb is generated by a tunable laser diode (TLD) centered at 1550.259 nm, followed by a DD-MZM, an optical PM and a single mode fiber (SMF) that compresses the optical pulse. The two cascaded modulators are driven both at B = 12.5 GHz. The peak to peak voltages, V_{ppi} (i = 1,2), at the outputs of the two RF driver amplifiers of the DD-MZM are 8.3 V and 11 V; the phase modulator is driven by a signal with 5.6 V peak to peak, to increase the overall modulation index.

It is important that the optical comb presents an adequate flatness, and that condition

$$\Delta A \pm \Delta\theta = \frac{\pi}{2}. \tag{6}$$

is satisfied [28]; here, $2\Delta A = \pi\left(V_{pp1} - V_{pp2}\right)\Big/\left(2V_{\pi}\right)$ is the phase difference between the RF signals and $2\Delta\theta$ is the phase difference between the DC bias [28]. The flexibility of the comb line allocation and the influence of the Gaussian pulse have been described in [29]. We underline the fact that the input pulse width should be shorter that the pulse interval in the OFDM symbol 1/(*B***N*). In our experiment, the comb is composed of seven lines with power fluctuation less than 1.9 dB as shown in Fig. 6(a) and the train of Gaussian pulses shown in Fig. 6(b) has 13-ps FWHM.

After the PM modulator, a 3-km SMF is used for pulse compression, an optical delay line (ODL) synchronizes the optical pulse peak with the electrical signal, and an erbium-doped fiber amplifier (EDFA) and an optical band pass filter (OBPF) are employed.

A DQPSK signal is obtained by precoding two 2^{15}-1 pseudo random data sequences (PRBS) for the in-phase (I) and quadrature (Q) signals, that are sent to a pulse pattern generator (PPG). The total optical power before the optical DQPSK modulator is 5 dBm, and the modulator insertion loss is 8 dB. All the optical comb lines are modulated by the same electrical signal, and the seven subcarriers are generated using a 3 dB coupler followed by two 6 dB couplers; variable optical attenuators (VOA) are used to equalize the subcarriers power, polarization controller (PC) and delay lines are used to decorrelate the seven optical signals. The lengths of the decorrelation delay lines are 1, 2, 3, 4 and 5 m. In this way, we achieve a

#233594 - $15.00 USD Received 29 Jan 2015; revised 30 Mar 2015; accepted 31 Mar 2015; published 20 Apr 2015

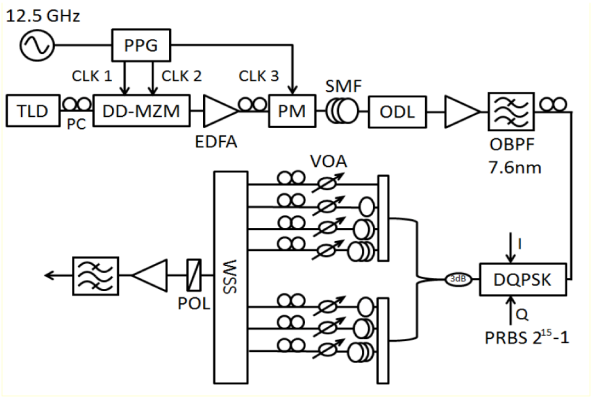

Fig. 5. Transmitter setup. Tunable laser diode (TLD), polarization controller (PC), dual-drive Mach-Zehnder (DD-MZM), pulse pattern generator (PPG), erbium-doped fiber amplifier (EDFA), clock (CLK), phase-modulator (PM), single mode fiber (SMF), optical delay line (ODL), optical band pass filter (OBPF), differential quadrature phase shift keying (DQPSK) modulator, variable optical attenuator (VOA), wavelength selective switch (WSS), polarization scrambling (POL), pseudo random bit sequence (PRBS).

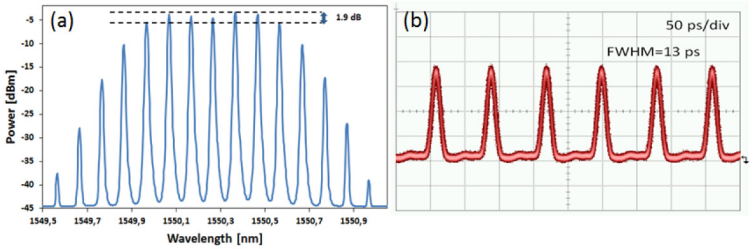

Fig. 6. (a) Measured optical comb. (b) Measured Gaussian pulses.

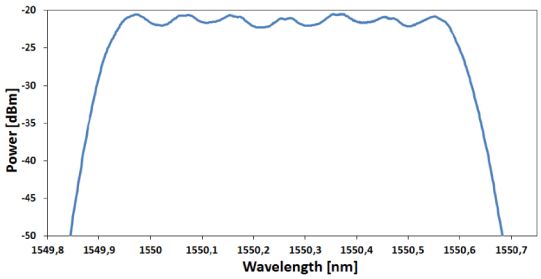

Fig. 7. Measured optical spectrum at the WSS output.

Full subcarrier decorrelation, and there is not ICI underestimation, as in the odd/even subcarriers approach [30].

A 1x8 WSS with 6 dB insertion loss is used at the TX; the measured transfer function for a single subcarrier is shown in Fig. 3 and the optical spectrum of the seven subcarriers is shown in Fig. 7. After the WSS we use a polarization scrambling (POL), an EDFA and a 7.6-nm OBPF. The total launched power to the SMF is 2 dBm.

Figure 8 shows the RX setup and the system performances are evaluated by attenuating the received power by a VOA, and splitting the signal with a 20-dB coupler before the AWG. The power meter (PWM) measures the 1% of the received power. The AWG has 16 ports, 200 GHz free spectral range (FSR), 12.5 GHz subcarrier spacing and 10 dB insertion loss. We

#233594 - $15.00 USD Received 29 Jan 2015; revised 30 Mar 2015; accepted 31 Mar 2015; published 20 Apr 2015

use a pre-amplifier, a 7.6-nm OBPF, a one-bit delay line interferometer (DLI) and a balanced photo-detector (BPD), with 45 GHz bandwidth, to measure the bit error rate (BER). The BER tester (BERT) supports line rates up to 32 Gb/s.

The measured eye diagrams for a seven channel system in B2B and after 35-km SMF are reported in Fig. 9(a) and 9(b); in this case log(BER) = −6. We remark that no optical time gating or chromatic dispersion compensation have been used. For a comparison, Fig. 10 shows the simulated eye diagrams of a single- and seven-channel transmission, in B2B case, and after 35-km SMF. The effect of ICI can be estimated by a comparison of Fig. 10, and also by an inspection of Fig. 11, where the spectrum at the AWG matched port is shown. Figure 11(a) reports the received spectrum at an AWG output port for a transmission of seven AO-OFDM subcarriers, and Fig. 11 (b) refers to the case when the target subcarrier is not transmitted, i.e. measures the ICI at the same port from the other six carriers. The measured crosstalk is −35.6 dBm.

Finally, Fig. 12 reports the BER measurements as a function of the total received power. The B2B behavior is compared with the performance obtained with the same setup, but using QPSK modulation and coherent detection. In case of coherent detection, five adjacent subcarriers, spaced 12.5 GHz each, are taken into account. DQPSK-modulated subcarrier in B2B presents about 3-dB penalty at BER = 10^{-6} with respect to coherent detection.

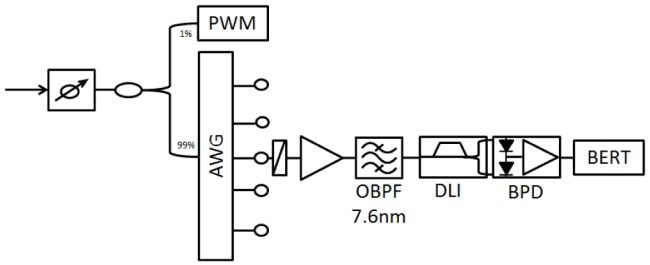

Fig. 8. Receiver setup. Power meter (PWM), arrayed waveguide grating (AWG), delay line interferometer (DLI), balanced photodetector (BPD), bit-error rate tester (BERT).

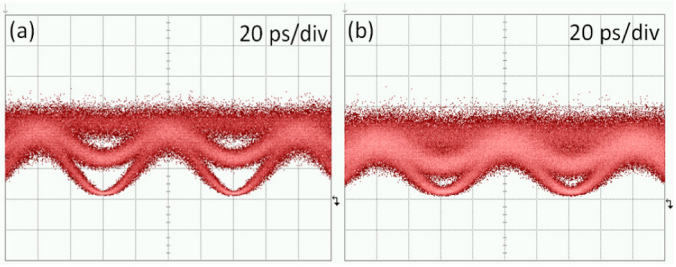

Fig. 9. Measured eye diagrams of a 7 ch-transmission (a) B2B (b) after 35-km SMF.

#233594 - $15.00 USD Received 29 Jan 2015; revised 30 Mar 2015; accepted 31 Mar 2015; published 20 Apr 2015

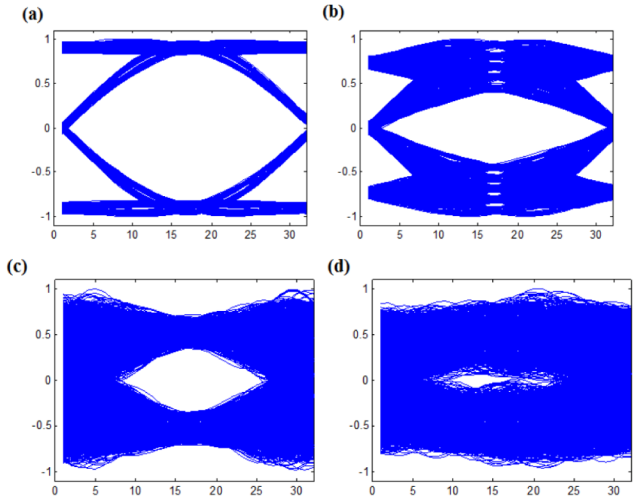

Fig. 10. Simulated eye diagrams (a) single channel B2B (b) single channel after 35-km SMF (c) seven channels B2B (d) seven channels after 35-km SMF.

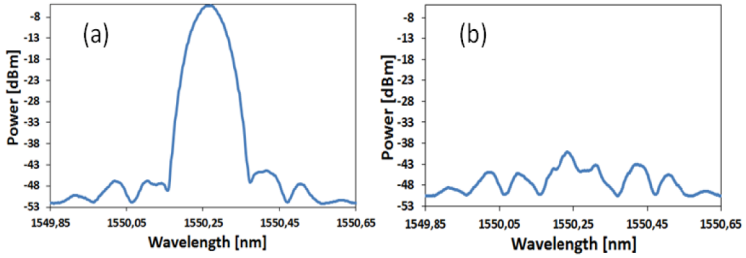

Fig. 11. Spectrum measured at an AWG output port (a) transmitting seven AO-OFDM carriers (b) transmitting six subcarriers (the target subcarrier has been switched off).

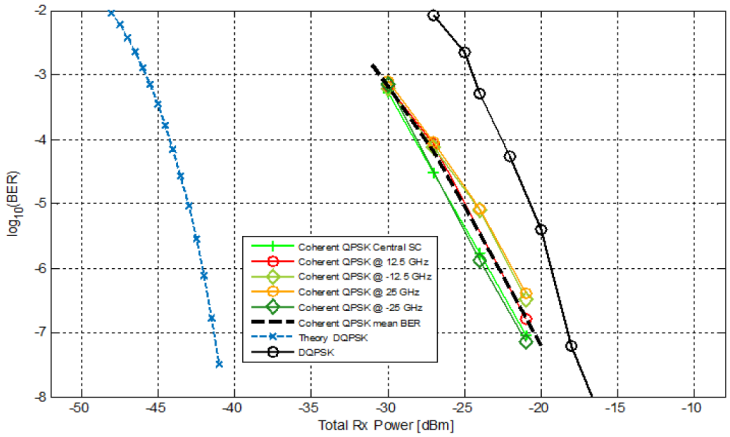

Fig. 12. BER vs received power in BTB for a DQPSK-modulated subcarrier received with direct detection compared with five QPSK subcarriers received by coherent detection (the dashed line corresponds to the mean BER curve of the five subcarriers). A theoretical curve for direct detection is also shown for reference.

#233594 - $15.00 USD Received 29 Jan 2015; revised 30 Mar 2015; accepted 31 Mar 2015; published 20 Apr 2015

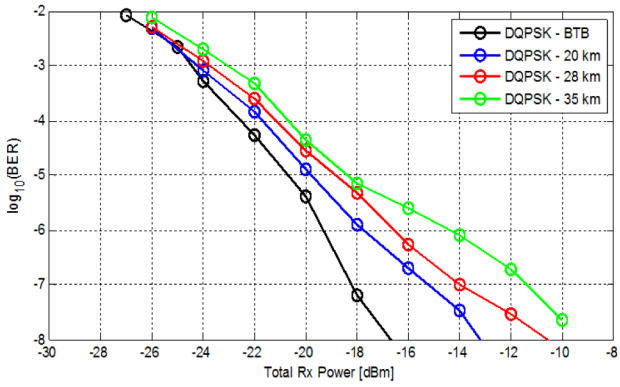

Fig. 13. BER vs received power for a DQPSK-modulated subcarrier for B2B, 20-km, 28-km, and 35-km transmission over uncompensated SMF.

Figure 13 reports BER measurements after 20-km, 28-km and 35-km SMF for the single DQSPK modulated subcarrier, without any dispersion compensation. Error-free transmission is achieved for all the subcarriers.

4. Conclusions

We have experimentally demonstrated error-free real-time transmission of seven DQPSK-modulated AO-OFDM subcarriers, using a WSS in the TX and an AWG at the RX. This configuration allows us to reduce ICI, when optical time gating is not applied and chromatic dispersion is not compensated. In addition, the use of the WSS at TX introduces flexibility in bandwidth assignment, whereas the AWG at the RX can simultaneously demultiplex a large number of subcarriers, presenting a better filtering behavior and maintaining the advantages of AO-OFDM in terms of cost and complexity.

Acknowledgments

This work was supported by the European Commission through ICT-ASTRON project (Contract No. 318714) funded under the 7th Framework Programme and the Italian Ministry of University and Research through ROAD-NGN project (PRIN2010-2011).

#233594 - $15.00 USD Received 29 Jan 2015; revised 30 Mar 2015; accepted 31 Mar 2015; published 20 Apr 2015